On the thermal conductivities of lithium ion conducting solid electrolytes

Thorben Böger[a,b], Tim Bernges[a], Yuheng Li[c], Pieremanuele Canepa[c,d,e],

Wolfgang G. Zeier*[a,b,f]

[a]*Institute of Inorganic and Analytical Chemistry, University of Münster, 48149 Münster, Germany*

[b]*International Graduate School for Battery Chemistry, Characterization, Analysis, Recycling and Application (BACCARA), University of Münster, 48149 Münster, Germany*

[c]*Department of Materials Science and Engineering, National University of Singapore, 117575, Singapore*

[d]*Department of Chemical and Biomolecular Engineering, National University of Singapore, 117585, Singapore*

[e]*Department of Electrical & Computer Engineering, University of Houston, TX, 77204, United States of America*

[f]*Forschungszentrum Jülich GmbH, Institute of Energy and Climate Research Helmholtz-Institute Münster (IEK-12), 52425 Jülich, Germany*

*Corresponding author email: wzeier@uni-muenster.de

Abstract

Solid electrolytes and solid-state batteries have gathered attention in recent years as a potential alternative to state-of-the-art lithium-ion batteries given the promised increased energy density and safety following the replacement of flammable organic electrolytes with solids. While ongoing research focuses mainly on improving the ionic conductivities of solid electrolytes, little is known about the thermal transport properties of this material class. This includes fundamental studies of heat capacities and thermal conductivities, and application-oriented investigations of porosity effects and the modeling of the temperature distribution in solid-state batteries during operation. To expand the understanding of transport in solid electrolytes, in this work, thermal properties of electrolytes in the argyrodite family (Li_6PS_5X with X = Cl, Br, I, and $Li_{5.5}PS_{4.5}Cl_{1.5}$) and $Li_{10}GeP_2S_{12}$ as a function of temperature and porosity are reported. It is shown that the thermal conductivities of solid electrolytes are in the range of liquid electrolytes. Utilizing effective medium theory to describe the porosity dependent results, an empirical predictive model is obtained and the intrinsic (bulk) thermal conductivities for all electrolytes are extracted. Moreover, the temperature-independent, glass-like thermal conductivities found in all materials suggest that thermal transport in these ionic conductors occurs in a non-textbook fashion.

Keywords

Thermal conductivity; solid electrolytes; solid-state batteries; effective medium theory; diffuson; ionic conductivity; phonon density of states;

1. Introduction

Lithium-ion batteries still represent the state-of-the-art battery technology. Nonetheless, in recent years, studies have paid increasing attention to solid-electrolytes and solid-state batteries as potential alternatives for conventional Li-ion battery systems.[1] In part, the interest in solid-state systems is facilitated by the discovery of promising Li^+ solid electrolytes of the $Li_{10}GeP_2S_{12}$ and argyrodite (Li_6PS_5X, X = halide) structural family that offer great compositional variety and exceptionally high ionic conductivities surpassing 5 mS cm^{-1}.[2–4] While ionic transport is well investigated in both material classes, there is limited understanding about their thermal transport properties,, which are expected to become increasingly important for safety considerations of solid-state batteries in potential large scale application in the future.[5,6]

Recent studies suggest that thermal conductivities of most solid-electrolytes, both, sulfide-[7,8] and oxide-based,[9,10] sulfides have low thermal conductivities (0.5 $Wm^{-1}K^{-1}$ to 1.5 $Wm^{-1}K^{-1}$) comparable to liquid carbonate-based electrolytes[11–13] (0.6 $Wm^{-1}K^{-1}$) used in conventional systems. Consequently, thermal management challenges in Li ion batteries that originate from poor heat dissipation (depending on the thermal conductivity) can be expected in solid-state systems as well.[6] For example, heat generated within a cell (or within a cell-stack) due to Joule heating needs to be transported through all components to reach the outer surface of the device where it can be dissipated, and where heat dissipation can be supported by passive or active cooling solutions.[14] With that, the rate at which heat is transferred in the system, as described by the thermal conductivity of the materials, becomes the decisive factor about the global and local temperature of the system.[15,16]

In the case of slow heat dissipation, the temperature of the battery increases with time. In moderation an increase of temperature can be beneficial considering, e.g., increased ionic conductivities or improved and more uniform lithium deposition at the lithium metal anode and the subsequent prevention of dendrites.[17,18] Nonetheless, at the same time, local heat accumulation can be detrimental by enhancing decomposition reactions, interphase formations, and in the worst case, by leading to thermal runaway.[19,20] Considering slow heat transport in solid electrolytes, the acclaimed safety of solid-state batteries is up to debate, especially since recent studies show that charged lithium nickel manganese cobalt oxide reacts violently with Li_6PS_5Cl already above 423 K.[19]

These safety considerations are intimately tied to the thermal properties of the battery components and consequently their characterization becomes increasingly important when solid-state batteries are brought from a laboratory to a commercialized scale.[21,22] With an outlook on increased amounts of active material and high current densities in these batteries stronger heat generation is expected (e.g., through increased Joule heating) that may make active cooling strategies a necessity in solid-state batteries. Modeling the generation and dissipation of heat under battery operation can be particularly helpful in answering some questions regarding battery safety.[6,16,23] However, these simulations require comprehensive knowledge of thermal transport properties, e.g., the heat capacity and thermal diffusivity of the battery materials that are rarely determined and discussed,[11,24] especially in solid state batteries[25]. Additionally, battery materials are generally not fully dense presenting a certain degree of porosity. Consequently, porosity, shown to have a strong effect on both, ionic[26,27] and thermal[8] transport in battery components, has to be considered and all measured transport quantities have to be treated as effective quantities.

While potential safety concerns motivate investigations of the thermal transport properties from an application viewpoint, there is also a fundamental interest in the transport behavior of fast ionic conductors. This is because the temperature-dependence of their thermal conductivities often deviates from the T^{-1} behavior[5] expected at elevated temperatures for phonon-gas like transport in crystalline solids.[28,29] This characteristic temperature dependence can be associated with Umklapp (phonon-phonon) scattering of propagating phonons that dominates over defect and grain-boundary scattering at elevated temperatures.[28] In contrast, many solid electrolytes show either a monotonous increase in thermal conductivity upon heating or a lack of any temperature dependence, characteristic for amorphous materials, despite their crystalline structure.[5] This unusual temperature dependence can be explained by phonons losing their plane-wave character in presence of strong anharmonicity and in absence of long-range order.[30] It was subsequently shown that significant portions of heat are conducted by so-called diffusons (non-plane-wave phonons) that exchange thermal energy in a random-walk fashion with other diffuson-type phonons.[31] Recently, this type of thermal transport was found to contribute in structurally complex or anharmonic materials as well, and given the glass-like thermal conductivity of Li_6PS_5Cl and other lithium solid electrolytes reported by Cheng et al.[7],

Neises et al.[10], and Bock et al.[32], it is likely that diffusons contribute to thermal transport in these material classes.

Inspired by the fundamental question of how heat is transported in solid electrolytes, and the subsequent question of how porosity influences heat transport with an outlook on future solid-state battery systems, this work investigates the temperature- and porosity-dependent thermal transport of a variety of Li^+ superionic conductors, spanning Li_6PS_5Cl, Li_6PS_5Br, Li_6PS_5I, $Li_{5.5}PS_{4.5}Cl_{1.5}$, as well as $Li_{10}GeP_2S_{12}$. Subsequently, the porosity dependence of the thermal conductivity (and diffusivity) is described by an effective medium model giving access to intrinsic material properties and offering an empirical predictive tool for future simulations of battery systems. Additionally, the temperature-dependent thermal conductivities are discussed from a viewpoint of diffuson-type transport of heat. Lastly, it is shown that the thermal and ionic conductivity are not macroscopically related, suggesting that independent engineering of both transport properties can be possible. Ultimately, this work provides a steppingstone and data framework for understanding and modeling heat dissipation in solid state batteries.

2. Results and discussion

Characterization of ionic transport. To evaluate potential trends or interrelations between the magnitude or temperature dependence of thermal and ionic transport, temperature-dependent impedance spectroscopy measurements were performed for all materials. A representative Nyquist plot of the impedance response of Li_6PS_5Cl at 233 K and the corresponding equivalent circuit fit are shown in Figure 1. The respective results for the other solid electrolytes can be found in the Supporting Information (Section S1, Figure S1). In agreement with literature reports[2,33–35], two processes (semicircles in the Nyquist representation) can be observed, with the first being attributed to the bulk resistance of the sample (capacitance of 20 pF), and the second being assigned to the grain-boundary resistance (capacitance of 0.69 nF) that is only resolved at low temperatures. Since bulk- and grain-boundary resistances can only be resolved for some materials at low temperatures, total ionic conductivities are discussed in the following. The temperature dependence of ionic transport in all solid electrolytes follows the expected Arrhenius behavior (Figure S2). In agreement with literature, Li_6PS_5I possesses the lowest ionic conductivity ($3.6 \cdot 10^{-3}$ mS cm^{-1} at room

temperature), while all other electrolytes exceed conductivities of 1 mS cm^{-1} at room temperature. The low magnitude of ion transport can be related to the lack of anion-site disorder in Li_6PS_5I leading to a strongly reduced intercage transport that is necessary for long-range ion diffusion.[33,35] Furthermore, the obtained activation energies (Figure 1b) are in good agreement with literature values for all investigated materials.[2,33–35] For detailed discussions of the ionic transport the reader is referred to reports in the literature on lithium argyrodites[33,35] and $Li_{10}GeP_2S_{12}$[2,36].

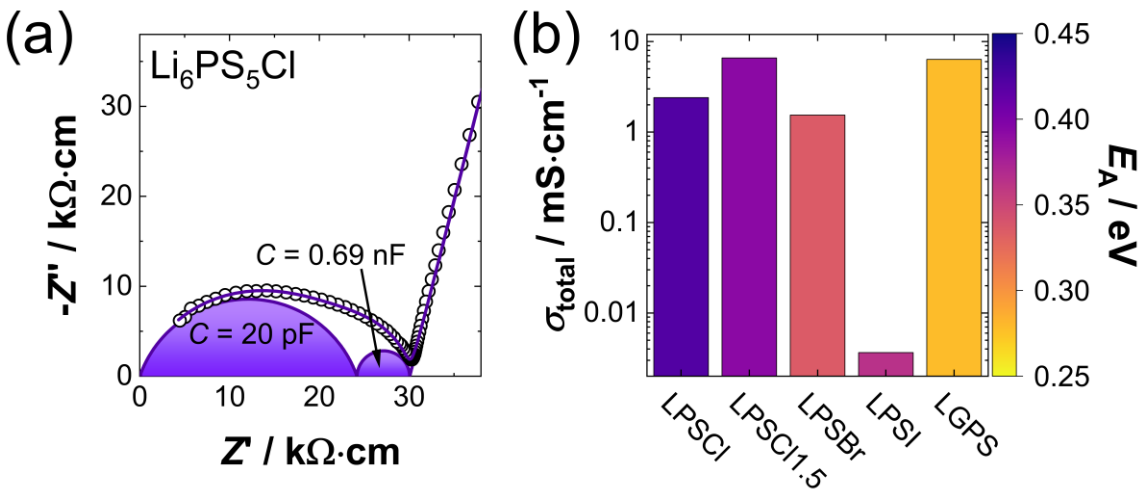

Figure 1. (a) Nyquist plot of the impedance response of Li_6PS_5Cl at 233 K, including the corresponding equivalent circuit (real and imaginary resistances normalized with respect to sample geometry). The first process (i.e., semicircle, red) can be attributed to the bulk resistance, whereas the second process (blue) is assigned to grain-boundary contributions. (b) Room temperature total conductivities of all investigated solid electrolytes Li_6PS_5Cl (LPSCl), $Li_{5.5}PS_{4.5}Cl_{1.5}$ (LPSCl1.5), Li_6PS_5Br (LPSBr), Li_6PS_5I (LPSI), and $Li_{10}GeP_2S_{12}$ (LGPS). The respective activation energies of all solid electrolytes are color-coded.

Characterization of thermal transport. To gain information about the thermal transport properties of the investigated solid electrolytes, initially, the thermal diffusivities are experimentally determined. Furthermore, the influence of porosity on transport is investigated by measurements on pellets of varying density, i.e., volume fraction of conductive material (solid electrolyte) in respect to the pellet volume. With that, the influence of temperature and porosity on thermal transport can be investigated. Due to the negligible density of the argon-filled pores, the volume fraction of solid electrolyte in the macroscopic sample can be approximated by its relative density.

All investigated materials show astonishingly low thermal diffusivities ranging from 0.15 $mm^2\ s^{-1}$ to 0.4 $mm^2\ s^{-1}$, as exemplary shown for Li_6PS_5Cl and $Li_{10}GeP_2S_{12}$ in Figure 2 a,c. All diffusivities show similar trends with temperature (Figure 2a and c, Figure S7), characterized by an initial decrease upon heating followed by approximately constant values above room temperature. As this change in temperature dependence (around room temperature) coincides with a detector change in the experiments (cf. Experimental section S2), a pyroceram reference sample was measured to rule out the possibility of a measurement artefact. Irrespective of the detector change, the measured values of the standard material are in accurate agreement with tabulated values. Consequently, the change in temperature dependence of the investigated solid electrolytes in fact originates from the materials themselves and not the measurement setup. The porosity dependence, i.e., the change of the volume fraction of conducting material, is characterized by a general decrease of the thermal diffusivity with increasing porosity (decreasing relative density). Later it is shown that this porosity-dependence can be described using an effective medium theory assuming thermally insulating pores.

Using the determined thermal diffusivities D, thermal conductivities κ can be calculated by multiplication with the specific isobaric heat capacity c_p and the sample density ρ following:

$$\kappa = c_p \cdot \rho \cdot D. \qquad 1$$

In distinction to the thermal diffusivities that quantify the diffusion of temperature, thermal conductivities describe the transport of energy in form of heat. In this work, the isobaric heat capacities are approximated by isochoric heat capacities obtained from the computed phonon density of states (Figures S3 and S4, details in Section S3). In general, the isobaric and isochoric heat capacities differ by a dilation term that is proportional to the bulk modulus of the material. Nonetheless, the bulk moduli of the investigated solid electrolytes are low (between 0.9 GPa[33] and 5.4 GPa[37]) so that, in first approximation, the dilation term remains negligible (details in Section S4).[38] Given the similarities between the computational heat capacities of Li_6PS_5Cl and Li_6PS_5I, the heat capacities of Li_6PS_5Br and $Li_{5.5}PS_{4.5}Cl_{1.5}$ are approximated based on the phonon calculations of Li_6PS_5Cl.

The heat capacities show the expected increase upon heating that saturates in the Dulong-Petit limit at elevated temperatures (Figure 2b and d, Figure S7). Especially at

low temperatures, the Dulong-Petit limit, assuming full excitation of all lattice vibrations, is not a good approximation and overestimates the heat capacities of solid-electrolytes.[28]

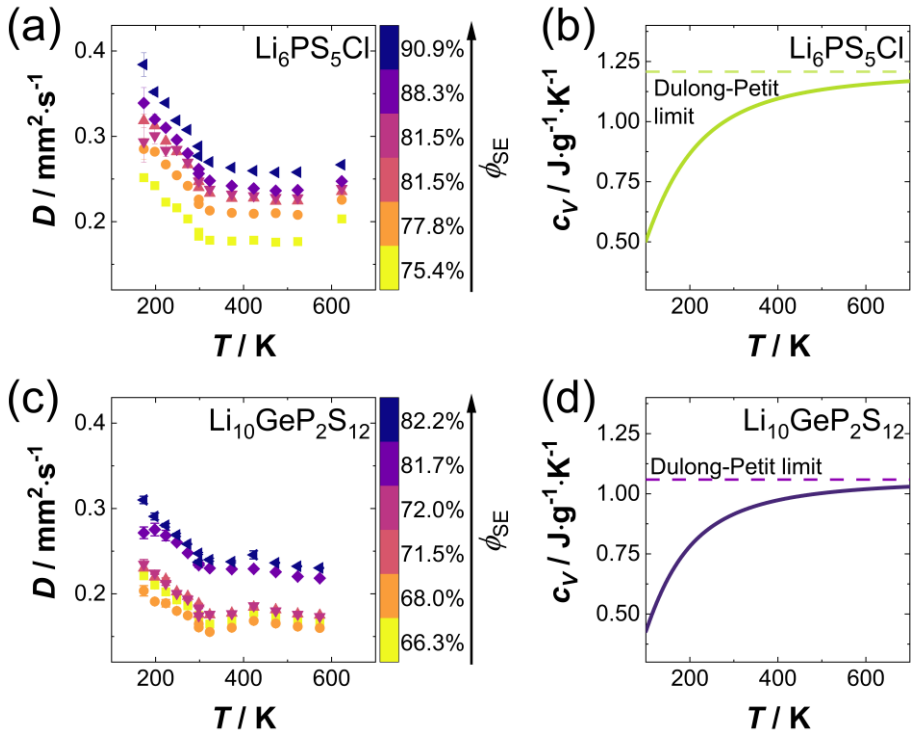

Figure 2. Temperature-dependent thermal diffusivities of (a) Li_6PS_5Cl and (c) $Li_{10}GeP_2S_{12}$ confirming the low magnitude of thermal diffusivity. The volume fractions of solid electrolyte (relative densities) are color coded. The respective (isochoric) heat capacities as a function of temperature are shown in (b), and (d) showing the expected increase with temperature and saturation to the Dulong-Petit limit at high temperatures. The heat capacity of $Li_{10}GeP_2S_{12}$ was calculated based on the phonon density of states reported in literature[39].

The thermal conductivities of Li_6PS_5Cl and $Li_{10}GeP_2S_{12}$, calculated using the isochoric specific heat and geometric density, are again exemplarily shown in Figure 3. The corresponding results of all solid electrolytes are shown in the Supporting Information (Figure S8). In agreement with the thermal diffusivities, all investigated electrolytes show astonishingly low thermal conductivities consistently below 1 W m^{-1} K^{-1} with almost no temperature dependence. This result corroborates other reports on sodium[8,9] and lithium[7,10] ionic conductors and strengthens the hypothesis of glass-, respectively diffuson-like, thermal transport in solid electrolytes. With that, the magnitudes of thermal conduction are not only comparable to but even below those of thermoelectric materials[40] and thermal barrier coating[41], specifically engineered for low

thermal conductivity. Moreover, the thermal conductivities of the solid electrolytes are within the same range as conventional carbonate-based liquid electrolytes (~0.6 W m^{-1} K^{-1}).[11–13] Hence, thermal management of solid-state batteries needs to take into account that the solid electrolytes, used as separator, as anolyte, and as catholyte, are poor thermal conductors resulting in slow dissipation of any heat generated during battery operation. The porosity (relative density) dependence of the thermal diffusivities persists to the thermal conductivities, with a general decrease of the thermal conductivity upon increasing the sample porosity. Therefore, densification of the solid electrolyte increases the rate of heat dissipation within a battery cell. The temperature dependence remains vastly untouched by this porosity dependence, so that changes to the sample relative density result only in an offset of the thermal conductivity magnitude.

While electrons can contribute to thermal conduction, the quasi-insulating nature of all solid electrolytes means that there are practically no contributions of electronic transport to thermal conductivity in these materials. Thus, the total thermal conductivity is equal to the lattice thermal conductivity contributed by phonon transport of heat. Moreover, there is also no primary transport of heat by mobile ions, which would lead to an increase of the thermal conductivity upon heating (following the activated ionic transport). Considering transition state theory[42], the contributions of mobile ions to the thermal conductivity are in the range of $3.3 \cdot 10^{-5}$ W m^{-1} K^{-1} to $4.0 \cdot 10^{-5}$ W m^{-1} K^{-1} at room temperature for the fastest investigated electrolytes $Li_{5.5}PS_{4.5}Cl_{1.5}$ and $Li_{10}GeP_2S_{12}$ (6.6 mS cm^{-1} and 6.4 mS cm^{-1} at room temperature, respectively. Details in Section S5). With that, the contributions of ion transport to thermal transport do not exceed 2% of the measured values, even at the highest investigated temperatures.[42]

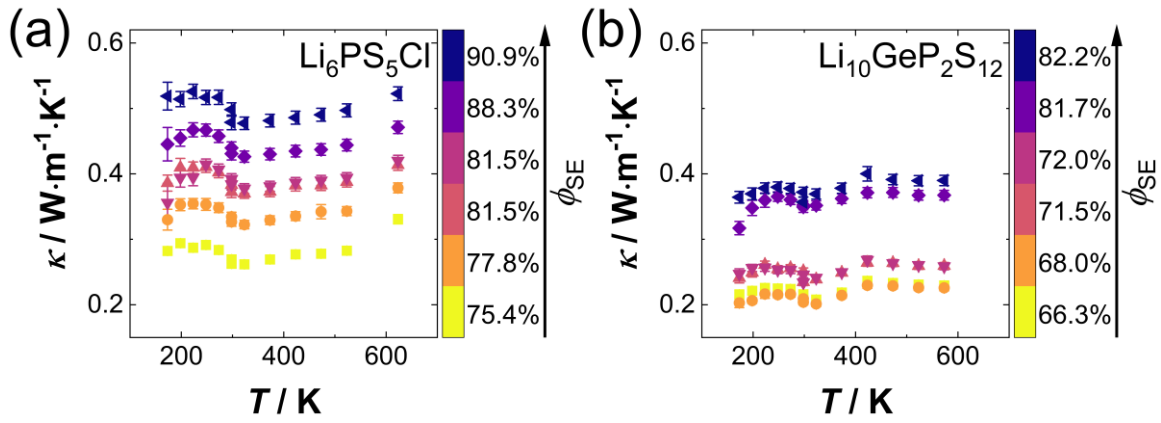

Figure 3. Temperature-dependent thermal conductivities for (a) Li_6PS_5Cl, and (b) $Li_{10}GeP_2S_{12}$ showing low magnitudes of thermal conductivity comparable to conventional electrolytes in Li ion batteries. The volume fractions of solid electrolyte (relative densities) are color coded. An increase of thermal conductivity with increasing volume fraction of solid electrolyte (decreasing porosity) is found.

Thermal conductivity with respect to relative density. Effective medium theory is a powerful tool to describe the transport properties and extract bulk properties from multi-component systems.[8,27] Generally, solid electrolytes and solid-state battery components represent at least two-phase systems composed of conducting material and (conducting or insulating) pores, as the materials are not fully dense in application. With that, transport properties, e.g., the thermal conductivity (Figure 4), are effective transport properties and influenced by the specimen porosity (or relative density). Different models have been developed to deduce properties of a composite or porous material from the respective volume fractions and the (intrinsic) properties of the pure materials. Maxwell[43], Eucken[44], Bruggeman[45], and others[46,47] developed suitable models (overview in Section S6) which have been subsequently improved to account for radiative[48] as well as interfacial thermal resistance[49]. For example, Bruggeman used differential effective medium theory to deduce the formula:[45]

$$\phi_{\mathrm{SE}} \frac{\kappa_{\mathrm{SE}} - \kappa_{\mathrm{eff}}}{\kappa_{\mathrm{SE}} + n \cdot \kappa_{\mathrm{eff}}} + (1 - \phi_{\mathrm{SE}}) \frac{\kappa_{\mathrm{g}} - \kappa_{\mathrm{eff}}}{\kappa_{\mathrm{g}} + n \cdot \kappa_{\mathrm{eff}}} = 0 \qquad 2$$

with the intrinsic thermal conductivities (i.e., at full densification) of the solid electrolyte and gaseous filler κ_{SE} and κ_g, respectively. The volume fraction of solid electrolyte is denoted by ϕ_{SE} and n is a shape factor characterizing the inclusions.

Using the assumptions of closed voids in the samples, no thermal conductivity due to convection can occur. Additionally, it is noted that the bulk thermal conductivity of the solid electrolyte κ_{SE} is much larger than that of the gaseous filler κ_g (in this case argon), justifying the negligence of thermal transport via pores.

With the assumptions mentioned above, Equation 2 can be further simplified yielding Equation 3. In the simplified Bruggeman equation, the effective thermal conductivity κ_{eff} is only a function of κ_{SE} and ϕ_{SE}, following:

$$\kappa_{\mathrm{eff}} = \kappa_{\mathrm{SE}} \phi_{\mathrm{SE}}^{(1+n)/n} = \kappa_{\mathrm{SE}} \phi_{\mathrm{SE}}^{\alpha}. \qquad 3$$

If the pores are spherical in shape, $n = 2$, and an exponent of $\alpha = 1.5$ is obtained.[45,47] While an exponent of 1.5 is the theoretical value for polydisperse, homogenously distributed spheres, in battery materials the exponent $\alpha = (1 + n)/n$ is often used as a fitting parameter to cope with more complex pore microstructures, e.g., to describe the partial ionic conductivities of cathode composites[27,50] or thermal transport in solid electrolytes[8] and batteries.[51]

By using α to fit the measured relative density-dependent thermal conductivities, the scaling of the thermal conductivity of all materials with density (porosity) can be described with high accuracy (shown for room temperature data, Figure 4). The Bruggeman exponents determined by fitting to the experimental data are in good agreement for all investigated materials, with an average of ~2.7 ± 0.2 at room temperature. Furthermore, the Bruggeman exponents show no significant temperature dependence (Figure S9), corresponding fits at 173 K and 523 K are shown in the Supporting Information (Figures S10 and S11). Constant Bruggeman exponents with temperature are not surprising given that they are in principle only dependent on the microstructure, i.e., the pore shape, which is not expected to change in the investigated temperature range.

Analogous fitting of the density dependent thermal diffusivities (Figure S12) leads to a reduced Bruggeman exponent (average for all materials ~1.6 ± 0.1) following that the thermal conductivities are obtained by multiplication of the diffusivities with the relative densities (details in Section S7). Therefore, the consistency of the Bruggemann exponents, between materials and with temperature, persists from the thermal conductivities to the thermal diffusivities. Moreover, the Bruggemann exponents obtained for the thermal diffusivities approximately match the expected value from the simplified assumption of homogenously dispersed spherical inclusion. Slight deviations from the idealized Bruggeman exponent of 1.5 for spherical pores are explained by the fact that neither the shape nor size of the crystallites are controlled and with that the pores are unlikely to be perfectly spherical. These deviations from the idealized spherical pore shape lead to an anisotropic geometry, which is related to higher Bruggeman exponents.[47] Nonetheless, the exponents of the thermal diffusivities closely match the approximations of the simplified model.

Careful characterization of the influence of porosity on transport has implications beyond the modelling of thermal conductivity, for instance to other transport properties

such as the ionic and electronic conductivities in solid electrolytes or cathode composites. Given the difficulties of accurately characterizing pore structures in macroscopic samples (and with that theoretically predicting Bruggeman exponents), Bruggeman exponents are commonly treated as fitting parameters to describe the density (porosity) dependencies of transport properties. In this work, we report the first empirical results from fitting of experimental data that give a predictive tool for thermal conductivities and diffusivities of important solid electrolyte classes. Thereby, we expect these results to guide the understanding of thermal transport in solid-state batteries. Despite the empirical nature of our result, the astonishing consistency of the Bruggeman exponents found in this work, without controlling or designing the microstructure of the material, motivates future studies focusing on the fundamental understanding of the influence of porosity on thermal conductivity.[52,53]

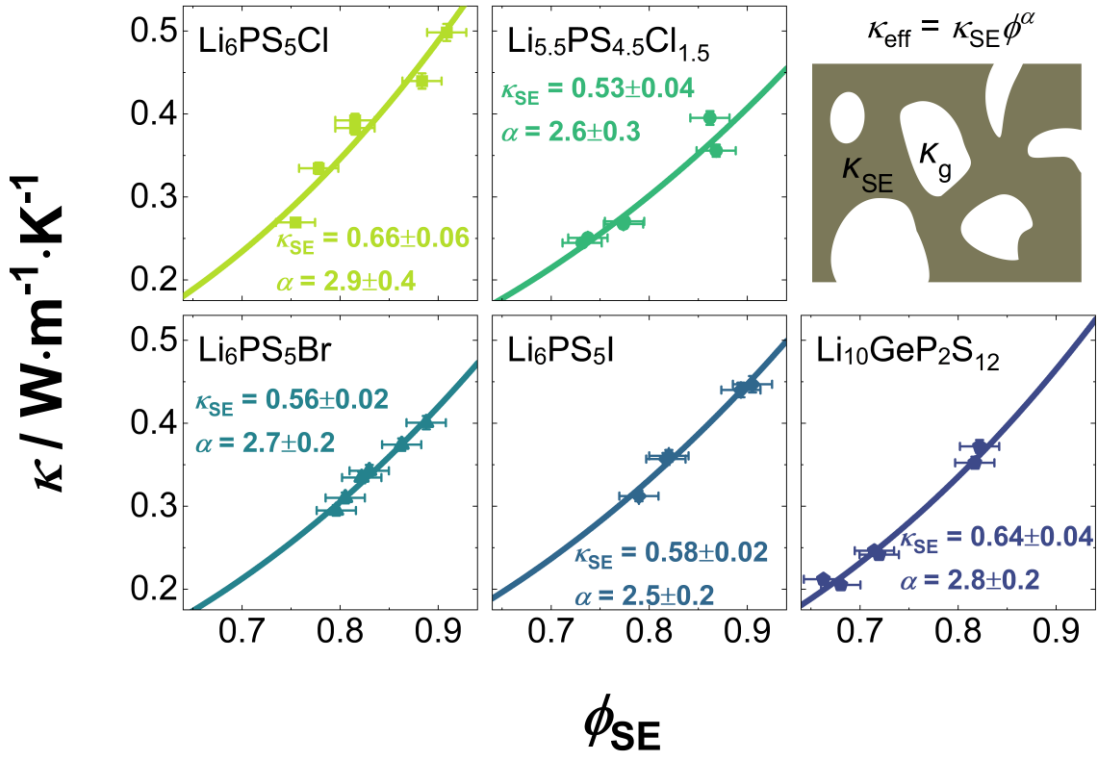

Figure 4. Volume fraction-dependent room-temperature thermal conductivity described by effective medium theory showing a consistent Bruggeman exponent α for all solid electrolytes. In the top right panel, an exemplary microstructure is shown with gas-filled pores in white and the solid electrolyte in brown, having thermal conductivities of κ_g and κ_{SE}, respectively.

Temperature dependence of thermal transport. While the scaling of thermal conductivity with porosity has significant importance considering application, the

magnitude and temperature dependence of κ_{SE} holds fundamental information about the underlying heat transport mechanism. To eliminate the influence of porosity on the discussion of thermal conductivity, the temperature-dependent thermal conductivities are extrapolated to full consolidation at all temperatures individually (Figure 5) using the described effective medium modeling approach. The thermal conductivity of Li_6PS_5Cl agrees well with values reported previously.[7] For all materials similar thermal conductivities above 400 K were found ranging between 0.50 W m^{-1} K^{-1} and 0.65 W m^{-1} K^{-1}, whereas at lower temperatures distinct temperature dependences are observed.

To understand the temperature dependencies, we first revisit the expected behavior of simple crystalline materials and glasses. Textbook thermal conductivity of crystalline solids is described by the so-called phonon-gas model[54], where phonons are treated as an ideal gas and propagate throughout the crystal until a scattering event occurs[28,29], e.g. at grain-boundaries, defects, or other phonons. Within the phonon-gas model, the thermal conductivity is directly proportional to the group velocity of the phonon branches, often approximated by the harmonic mean speed of sound, the isochoric heat capacity, and the mean-free path between two scattering events.[28] In contrast, in glasses, due to their lack of long-range order and the subsequent difficulties to define plane waves, phonons often cannot be described sufficiently from a phonon-gas viewpoint.[55] Consequently, a second type of phonons, the so-called “diffuson”, is introduced to describe the thermal transport in amorphous materials, whose heat transport resembles a random-walk of thermal energy by coupling of vibrational modes.[54,56] Multiple studies show that not only glasses but also specific crystalline materials with strong structural complexity or pronounced anharmonicity such as $Yb_{14}(Mn,Mg)Sb_{11}$[56], $Ag_8Ge_{1-x}(Si,Sn)_xSe_6$[57], $Ag_9Ge_{1-x}Ga_xSe_6$[58], $Y_{1-x}Nb_xO_{1.5+x}$[59], $Cs_3Bi_2I_6Cl_3$[60], different skutterudites[61], or $Bi_2Sr_2(Ca,Y)Cu_2O_8$[62] exhibit contributions of diffuson transport.

The phonon-gas and the diffuson models show opposing temperature dependences. While phonon-phonon interactions of propagating phonons (phonon-gas model) lead to a typical T^{-1}-dependence above the Debye temperature, diffuson contributions to the thermal conductivity increase upon heating and saturate at high temperatures. Although the onset of both patterns is highly material dependent, both transport mechanisms can in principle be distinguished by the temperature dependence of the thermal conductivities. Interestingly, the thermal conductivities of the solid electrolytes

measured in this study show either a lack of temperature dependence or an increase of thermal conductivity upon heating, indicative of diffuson transport (Figure 5). This becomes especially clear when comparing the data to reference lines showing the expected T^{-1}-behavior of phonon-gas transport and the increasing and saturating behavior from diffuson transport (Figure 5, details in Section S8).

While increasing thermal conductivities are observed for Li_6PS_5I, in the other samples the thermal conductivity shows nearly temperature independence, thereby significantly deviating from the expected temperature dependence of both, phonon-gas and diffuson-like transport below 400 K (Figure 5). This deviation can be explained from a "two-channel" perspective, where both, phonon-gas- and diffuson-like transport have significant contributions to the overall thermal conductivity. In this case, contributions from phonon-gas transport with decreasing, and diffuson transport with increasing thermal conductivity contributions, compensate and lead to the persistence of a flat temperature dependence to lower temperatures. This behavior, resulting from two-channel transport, has been shown previously in the Ag^+ analogous of the argyrodites, e.g., Ag_8GeSe_6[57] and Ag_9GaSe_6[58], and our experimental results suggest that it prevails over lithium argyrodites and $Li_{10}GeP_2S_{12}$. At this point it is not possible to corroborate this hypothesis quantitatively, since measurements of the thermal conductivity to even lower temperatures (< 10 K)[60] are necessary that are challenging given the moisture sensitivity of the investigated electrolytes. Nonetheless, the almost temperature independent and low-magnitude thermal conductivities observed in all solid electrolytes studied here strongly suggests significant diffuson-contributions to thermal transport in agreement with the observation of glass-like thermal conduction in fast ionic conductors in the literature[7,8,10].

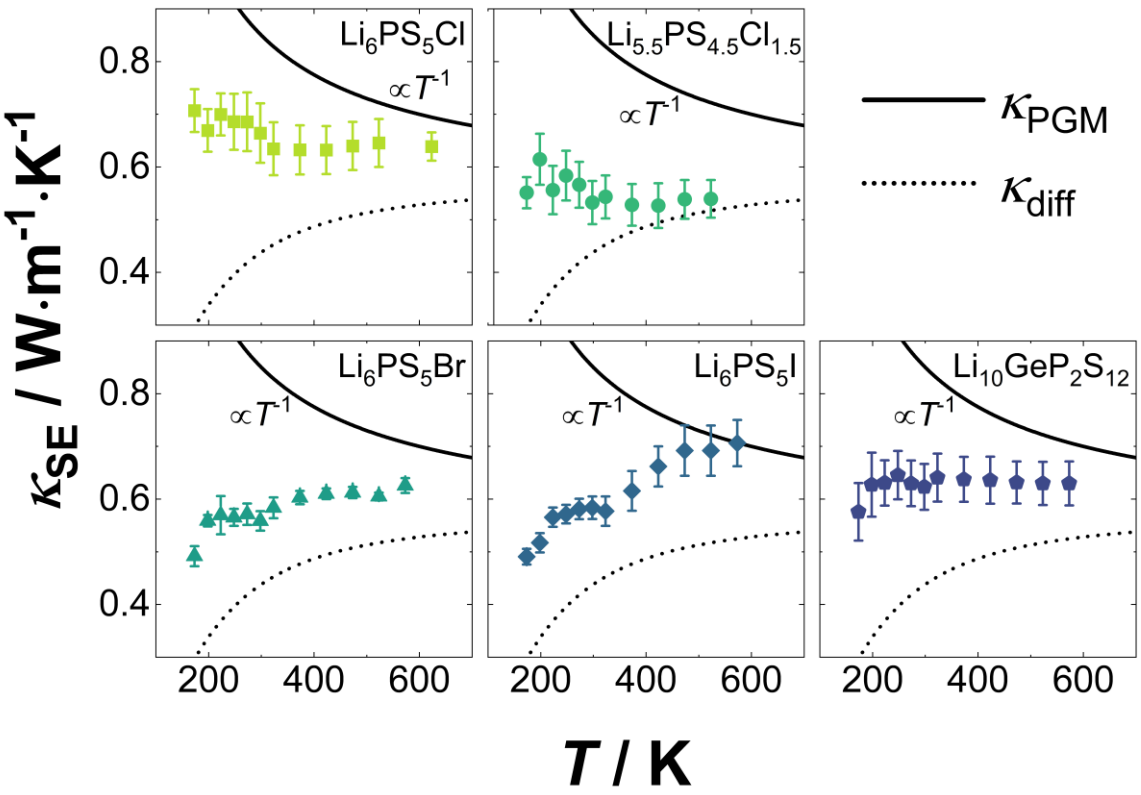

Figure 5. Temperature-dependent bulk (intrinsic) thermal conductivities of all investigated solid electrolytes. Reference lines indicate the expected temperature dependencies of diffuson-like (κ_{diff}) and phonon-gas-like (κ_{PGM}) transport. The weak temperature dependencies expected to be caused by the mutual compensation of the thermal conductivity contributions of both transport mechanisms.

Comparing ionic and thermal conduction. Recently, it was suggested that the simultaneous presence of low thermal and high ionic transport is not coincidental, but a result of the shared dynamic and/or structural features of fast ionic conduction and glass-like (diffuson) thermal conduction, e.g., overall soft dynamics (low force constants)[63,64], complex and hierarchical bonding[65], and strong anharmonicity[64,66]. While a microscopic understanding and verification of the hypothesized shared foundation needs further study, a potential macroscopic relation is evaluated by comparing the thermal and ionic conductivity.

Comparing the magnitude and temperature dependence (Figure 6) of both transport properties it can be seen that no macroscopic correlation exists, with the ionic conductivity varying up to two orders of magnitude within one compound upon heating from 233 K to 333 K, while the thermal conductivity stays approximately constant. The increase in ionic conduction is caused by its activated Boltzmann-like transport, with

activation barriers of 290 meV to 410 meV. In comparison, the thermal energy ($k_B T$) in the investigated temperature range ranges from 20 meV to 30 meV.

In contrast, the studied solid electrolytes are characterized by soft lattice dynamics, meaning that phonons possess low energies below 70 meV. Considering that the majority of heat is carried by phonons of very low energy[56,57], no pronounced activated behavior is observed, as a majority of phonons is already (thermally) excited at intermediate temperatures.

Even larger differences of more than five orders of magnitude are observed when comparing the ionic conductivities of all compounds, while at the same time the thermal conductivities vary by only ~50%. This can be explained by the fact that subtle structural changes directly impact the diffusion pathway of the mobile ions[67], while at the same time, they do not significantly change the average force constants (phonon energies) and with that the heat transport by phonons.[64]

Despite the lack of a direct correlation between the magnitudes of ionic and thermal transport, a general and important observation is that all solid electrolytes investigated here and in the literature[5] show low magnitudes of thermal conductivity, raising concerns about potential challenges in thermal management of solid-state batteries. However, the lack of a macroscopic correlation between both transport phenomena leaves the possibility open that both transport properties can be manipulated and designed independently. Therefore, attempts can be made to engineer battery materials to have higher thermal conductivities, i.e., improved heat dissipation, without negatively influencing the ionic conductivity.

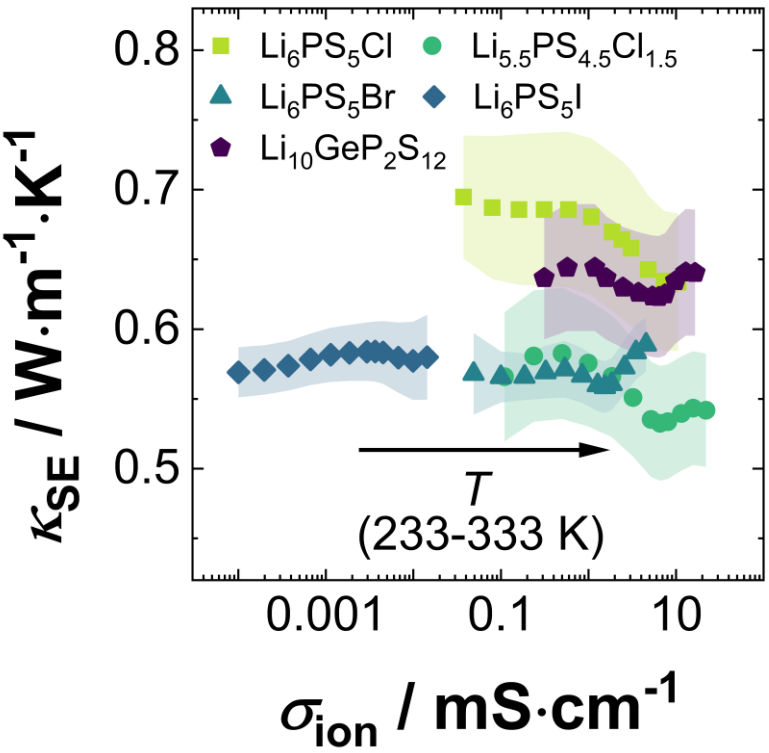

Figure 6. Comparison of ionic and thermal transport showing no macroscopic correlation between both quantities. Shaded areas represent the uncertainty in thermal conductivity. Due to the nature of being a thermally activated process and its sensitivity to lattice site occupations, the ionic conductivities span approximately six orders of magnitude across all compositions, while changes of the thermal conductivity are contained within one order of magnitude.

3. Conclusion

In this work, the porosity dependence of the thermal conductivities of four different argyrodites (Li_6PS_5X with X = Cl, Br, I, and $Li_{5.5}PS_{4.5}Cl_{1.5}$) and $Li_{10}GeP_2S_{12}$ were investigated and described by effective medium theory. With that, a predictive empirical model for the scaling behavior of thermal conduction is presented that can support simulations concerning the thermal management of solid-state batteries. Additionally, the temperature dependence of the thermal conductivities strongly suggests two-channel thermal transport, with contributions by both, phonon-gas and diffuson-like transport, motivating further studies focusing on the fundamental understanding of transport in ionic conductors. Based on this work, the magnitude and temperature dependence of ionic and thermal transport are not directly related suggesting possibilities to tune both properties independently.

Supporting Information

Nyquist and Arrhenius plots; experimental section; discussion of phonon density of states; details on calculation of heat capacity; thermal conductivity by ions; comparison of effective medium theories; further discussion of Bruggeman theory; model of diffuson-like thermal transport; structural analysis

Acknowledgments

Th.B. is member of the International Graduate School for Battery Chemistry, Characterization, Analysis, Recycling and Application (BACCARA), which is funded by the Ministry for Culture and Science of North Rhine Westphalia, Germany. The simulations for this work were performed on the computer cluster PALMA II of the University of Münster.

Author Contributions

CRediT: **Thorben Böger** Conceptualization, Validation, Formal analysis, Investigation, Data Curation, Writing - Original Draft, Visualization. **Tim Bernges** Conceptualization, Methodology, Writing - Review & Editing. **Yuheng Li** Validation, Data Curation **Pieremanuele Canepa** Validation, Data Curation. **Wolfgang G. Zeier** Conceptualization, Resources, Writing - Review & Editing, Supervision.

Notes

The authors declare no competing financial interest. The data that support the findings of this study are available from the corresponding author, W. Z., upon reasonable request.

References

(1) Janek, J.; Zeier, W. G. Challenges in speeding up solid-state battery development. *Nat. Energy* **2023**, *8* (3), 230–240. DOI: 10.1038/s41560-023-01208-9.

(2) Kato, Y.; Hori, S.; Kanno, R. Li10GeP2S12 -Type Superionic Conductors: Synthesis, Structure, and Ionic Transportation. *Adv. Energy Mater.* **2020**, *10* (42), 2002153. DOI: 10.1002/aenm.202002153.

(3) Wang, S.; Gautam, A.; Wu, X.; Li, S.; Zhang, X.; He, H.; Lin, Y.; Shen, Y.; Nan, C.-W. Effect of Processing on Structure and Ionic Conductivity of Chlorine-Rich Lithium

Argyrodites. *Adv Energy and Sustain Res* **2023**, 2200197. DOI: 10.1002/aesr.202200197.

(4) Adeli, P.; Bazak, J. D.; Park, K. H.; Kochetkov, I.; Huq, A.; Goward, G. R.; Nazar, L. F. Boosting Solid-State Diffusivity and Conductivity in Lithium Superionic Argyrodites by Halide Substitution. *Angew. Chem. Int. Ed. Engl.* **2019**, *58* (26), 8681–8686. DOI: 10.1002/anie.201814222. Published Online: May. 24, 2019.

(5) Agne, M. T.; Böger, T.; Bernges, T.; Zeier, W. G. Importance of Thermal Transport for the Design of Solid-State Battery Materials. *PRX Energy* **2022**, *1* (3), 31002. DOI: 10.1103/PRXEnergy.1.031002.

(6) Vishnugopi, B. S.; Hasan, M. T.; Zhou, H.; Mukherjee, P. P. Interphases and Electrode Crosstalk Dictate the Thermal Stability of Solid-State Batteries. *ACS Energy Lett.* **2023**, *8* (1), 398–407. DOI: 10.1021/acsenergylett.2c02443.

(7) Cheng, Z.; Zahiri, B.; Ji, X.; Chen, C.; Chalise, D.; Braun, P. V.; Cahill, D. G. Good Solid-State Electrolytes Have Low, Glass-Like Thermal Conductivity. *Small* **2021**, *17* (28), e2101693. DOI: 10.1002/smll.202101693. Published Online: Jun. 12, 2021.

(8) Bernges, T.; Böger, T.; Maus, O.; Till, P. S.; Agne, M. T.; Zeier, W. G. Scaling Relations for Ionic and Thermal Transport in the Na+ Ionic Conductor Na3PS4. *ACS Materials Lett.* **2022**, 2491–2498. DOI: 10.1021/acsmaterialslett.2c00846.

(9) Rohde, M.; Mohsin, I. U. I.; Ziebert, C.; Seifert, H. J. Ionic and Thermal Transport in Na-Ion-Conducting Ceramic Electrolytes. *Int. J. Thermophys.* **2021**, *42* (10), 136. DOI: 10.1007/s10765-021-02886-x.

(10) Neises, J.; Scheld, W. S.; Seok, A.-R.; Lobe, S.; Finsterbusch, M.; Uhlenbruck, S.; Schmechel, R.; Benson, N. Study of thermal material properties for Ta- and Al-substituted Li7La3Zr2O12 (LLZO) solid-state electrolyte in dependency of temperature and grain size. *J. Mater. Chem. A* **2022**, *10* (22), 12177–12186. DOI: 10.1039/D2TA00323F.

(11) Chen, S. C.; Wan, C. C.; Wang, Y. Y. Thermal analysis of lithium-ion batteries. *J. Power Sources* **2005**, *140* (1), 111–124. DOI: 10.1016/j.jpowsour.2004.05.064.

(12) Cheng, L.; Ke, C.; Fengchun, S.; Peng, T.; Hongwei, Z. Research on thermo-physical properties identification and thermal analysis of EV Li-ion battery. In *2009 IEEE Vehicle Power and Propulsion Conference*; IEEE, 2009; pp 1643–1648. DOI: 10.1109/VPPC.2009.5289653.

(13) Wei, L.; Lu, Z.; Cao, F.; Zhang, L.; Yang, X.; Yu, X.; Jin, L. A comprehensive study on thermal conductivity of the lithium-ion battery. *Int. J. Energy Res.* **2020**, *44* (12), 9466–9478. DOI: 10.1002/er.5016.

(14) Patel, J. R.; Rathod, M. K. Recent developments in the passive and hybrid thermal management techniques of lithium-ion batteries. *J. Power Sources* **2020**, *480*, 228820. DOI: 10.1016/j.jpowsour.2020.228820.

(15) Kunz, A.; Berg, C.; Friedrich, F.; Gasteiger, H. A.; Jossen, A. Time-Resolved Electrochemical Heat Flow Calorimetry for the Analysis of Highly Dynamic Processes in Lithium-Ion Batteries. *J. Electrochem. Soc.* **2022**, *169* (8), 80513. DOI: 10.1149/1945-7111/ac8625.

(16) Steinhardt, M.; Gillich, E. I.; Stiegler, M.; Jossen, A. Thermal conductivity inside prismatic lithium-ion cells with dependencies on temperature and external compression pressure. *J. Energy Storage* **2020**, *32*, 101680. DOI: 10.1016/j.est.2020.101680.

(17) Gao, X.; Zhou, Y.-N.; Han, D.; Zhou, J.; Zhou, D.; Tang, W.; Goodenough, J. B. Thermodynamic Understanding of Li-Dendrite Formation. *Joule* **2020**, *4* (9), 1864–1879. DOI: 10.1016/j.joule.2020.06.016.

(18) Krauskopf, T.; Richter, F. H.; Zeier, W. G.; Janek, J. Physicochemical Concepts of the Lithium Metal Anode in Solid-State Batteries. *Chem. Rev.* **2020**, *120* (15), 7745–7794. DOI: 10.1021/acs.chemrev.0c00431. Published Online: Jul. 27, 2020.

(19) Kim, T.; Kim, K.; Lee, S.; Song, G.; Jung, M. S.; Lee, K. T. Thermal Runaway Behavior of Li6PS5Cl Solid Electrolytes for LiNi0.8Co0.1Mn0.1O2 and LiFePO4 in All-Solid-State Batteries. *Chem. Mater.* **2022**, *34* (20), 9159–9171. DOI: 10.1021/acs.chemmater.2c02106.

(20) Banerjee, A.; Wang, X.; Fang, C.; Wu, E. A.; Meng, Y. S. Interfaces and Interphases in All-Solid-State Batteries with Inorganic Solid Electrolytes. *Chem. Rev.* **2020**, *120* (14), 6878–6933. DOI: 10.1021/acs.chemrev.0c00101. Published Online: Jun. 30, 2020.

(21) Kim, J.; Oh, J.; Lee, H. Review on battery thermal management system for electric vehicles. *Appl. Therm. Eng.* **2019**, *149*, 192–212. DOI: 10.1016/j.applthermaleng.2018.12.020.

(22) Shahjalal, M.; Shams, T.; Islam, M. E.; Alam, W.; Modak, M.; Hossain, S. B.; Ramadesigan, V.; Ahmed, M. R.; Ahmed, H.; Iqbal, A. A review of thermal

management for Li-ion batteries: Prospects, challenges, and issues. *J. Energy Storage* **2021**, *39*, 102518. DOI: 10.1016/j.est.2021.102518.

(23) Kraft, L.; Hoefling, A.; Zünd, T.; Kunz, A.; Steinhardt, M.; Tübke, J.; Jossen, A. Implications of the Heat Generation of LMR-NCM on the Thermal Behavior of Large-Format Lithium-Ion Batteries. *J. Electrochem. Soc.* **2021**, *168* (5), 53505. DOI: 10.1149/1945-7111/ac0069.

(24) Maleki, H.; Hallaj, S. A.; Selman, J. R.; Dinwiddie, R. B.; Wang, H. Thermal Properties of Lithium-Ion Battery and Components. *J. Electrochem. Soc.* **1999**, *146* (3), 947–954. DOI: 10.1149/1.1391704.

(25) Johnson, N.; Albertus, P. Modeling Thermal Behavior and Safety of Large Format All-Solid-State Lithium Metal Batteries under Thermal Ramp and Short Circuit Conditions. *J. Electrochem. Soc.* **2022**, *169* (6), 60546. DOI: 10.1149/1945-7111/ac79cf.

(26) Bielefeld, A.; Weber, D. A.; Janek, J. Modeling Effective Ionic Conductivity and Binder Influence in Composite Cathodes for All-Solid-State Batteries. *ACS Appl. Mater. Interfaces* **2020**, *12* (11), 12821–12833. DOI: 10.1021/acsami.9b22788. Published Online: Mar. 5, 2020.

(27) Dewald, G. F.; Ohno, S.; Hering, J. G. C.; Janek, J.; Zeier, W. G. Analysis of Charge Carrier Transport Toward Optimized Cathode Composites for All-Solid-State Li−S Batteries. *Batteries Supercaps* **2021**, *4* (1), 183–194. DOI: 10.1002/batt.202000194.

(28) Hunklinger, S.; Enss, C., Eds. *Solid State Physics*; De Gruyter, 2022. DOI: 10.1515/9783110666502.

(29) Toberer, E. S.; Zevalkink, A.; Snyder, G. J. Phonon engineering through crystal chemistry. *J. Mater. Chem.* **2011**, *21* (40), 15843. DOI: 10.1039/c1jm11754h.

(30) Allen; Feldman. Thermal conductivity of glasses: Theory and application to amorphous Si. *Phys. Rev. Lett.* **1989**, *62* (6), 645–648. DOI: 10.1103/PhysRevLett.62.645.

(31) Allen, P. B.; Feldman, J. L.; Fabian, J.; Wooten, F. Diffusons, locons and propagons: Character of atomic vibrations in amorphous Si. *Philos. Mag. B* **1999**, *79* (11-12), 1715–1731. DOI: 10.1080/13642819908223054.

(32) Bock, R.; Onsrud, M.; Karoliussen, H.; Pollet, B.; Seland, F.; Burheim, O. Thermal Gradients with Sintered Solid State Electrolytes in Lithium-Ion Batteries. *Energies* **2020**, *13* (1), 253. DOI: 10.3390/en13010253.

(33) Kraft, M. A.; Culver, S. P.; Calderon, M.; Böcher, F.; Krauskopf, T.; Senyshyn, A.; Dietrich, C.; Zevalkink, A.; Janek, J.; Zeier, W. G. Influence of Lattice Polarizability on the Ionic Conductivity in the Lithium Superionic Argyrodites Li6PS5X (X = Cl, Br, I). *J. Am. Chem. Soc.* **2017**, *139* (31), 10909–10918. DOI: 10.1021/jacs.7b06327. Published Online: Jul. 28, 2017.

(34) Gautam, A.; Ghidiu, M.; Suard, E.; Kraft, M. A.; Zeier, W. G. On the Lithium Distribution in Halide Superionic Argyrodites by Halide Incorporation in Li7-xPS6-xClx. *ACS Appl. Energy Mater.* **2021**, *4* (7), 7309–7315. DOI: 10.1021/acsaem.1c01417.

(35) Rayavarapu, P. R.; Sharma, N.; Peterson, V. K.; Adams, S. Variation in structure and Li+-ion migration in argyrodite-type Li6PS5X (X = Cl, Br, I) solid electrolytes. *J. Solid State Electrochem.* **2012**, *16* (5), 1807–1813. DOI: 10.1007/s10008-011-1572-8.

(36) Kamaya, N.; Homma, K.; Yamakawa, Y.; Hirayama, M.; Kanno, R.; Yonemura, M.; Kamiyama, T.; Kato, Y.; Hama, S.; Kawamoto, K.; Mitsui, A. A lithium superionic conductor. *Nat. Mater.* **2011**, *10* (9), 682–686. DOI: 10.1038/nmat3066. Published Online: Jul. 31, 2011.

(37) Weber, D. A.; Senyshyn, A.; Weldert, K. S.; Wenzel, S.; Zhang, W.; Kaiser, R.; Berendts, S.; Janek, J.; Zeier, W. G. Structural Insights and 3D Diffusion Pathways within the Lithium Superionic Conductor Li10GeP2S12. *Chem. Mater.* **2016**, *28* (16), 5905–5915. DOI: 10.1021/acs.chemmater.6b02424.

(38) Agne, M. T.; Imasato, K.; Anand, S.; Lee, K.; Bux, S. K.; Zevalkink, A.; Rettie, A. J.; Chung, D. Y.; Kanatzidis, M. G.; Snyder, G. J. Heat capacity of Mg3Sb2, Mg3Bi2, and their alloys at high temperature. *Mater. Today Phys.* **2018**, *6*, 83–88. DOI: 10.1016/j.mtphys.2018.10.001.

(39) Xu, Z.; Chen, X.; Zhu, H.; Li, X. Anharmonic Cation-Anion Coupling Dynamics Assisted Lithium-Ion Diffusion in Sulfide Solid Electrolytes. *Adv. Mater.* **2022**, *34* (49), e2207411. DOI: 10.1002/adma.202207411. Published Online: Oct. 31, 2022.

(40) Tian, Z.; Lee, S.; Chen, G. A Comprehensive Review of Heat Transfer in Thermoelectric Materials and Devices. *arXiv* **2014**, 1–64. DOI: 10.48550/arXiv.1401.0749.

(41) Clarke, D. R. Materials selection guidelines for low thermal conductivity thermal barrier coatings. *Surf. Coat. Technol.* **2003**, *163-164*, 67–74. DOI: 10.1016/S0257-8972(02)00593-5.

(42) Rice, M. J.; Roth, W. L. Ionic transport in super ionic conductors: a theoretical model. *J. Solid State Chem.* **1972**, *4* (2), 294–310. DOI: 10.1016/0022-4596(72)90121-1.

(43) Pietrak, K.; Wiśniewski, T. S. A review of models for effective thermal conductivity of composite materials. *J. Power Technol.* **2015**, *95* (1), 14–24.

(44) Carson, J. K.; Lovatt, S. J.; Tanner, D. J.; Cleland, A. C. Thermal conductivity bounds for isotropic, porous materials. *Int. J. Heat Mass Transfer* **2005**, *48* (11), 2150–2158. DOI: 10.1016/j.ijheatmasstransfer.2004.12.032.

(45) Tjaden, B.; Cooper, S. J.; Brett, D. J. L.; Kramer, D.; Shearing, P. R. On the origin and application of the Bruggeman correlation for analysing transport phenomena in electrochemical systems. *Curr. Opin. Chem. Eng.* **2016**, *12*, 44–51. DOI: 10.1016/j.coche.2016.02.006.

(46) Gong, L.; Wang, Y.; Cheng, X.; Zhang, R.; Zhang, H. A novel effective medium theory for modelling the thermal conductivity of porous materials. *Int. J. Heat Mass Transfer* **2014**, *68*, 295–298. DOI: 10.1016/j.ijheatmasstransfer.2013.09.043.

(47) Cernuschi, F.; Ahmaniemi, S.; Vuoristo, P.; Mäntylä, T. Modelling of thermal conductivity of porous materials: application to thick thermal barrier coatings. *J. Eur. Ceram. Soc.* **2004**, *24* (9), 2657–2667. DOI: 10.1016/j.jeurceramsoc.2003.09.012.

(48) Kiradjiev, K. B.; Halvorsen, S. A.; van Gorder, R. A.; Howison, S. D. Maxwell-type models for the effective thermal conductivity of a porous material with radiative transfer in the voids. *Int. J. Therm. Sci.* **2019**, *145*, 106009. DOI: 10.1016/j.ijthermalsci.2019.106009.

(49) Nan, C.-W.; Birringer, R.; Clarke, D. R.; Gleiter, H. Effective thermal conductivity of particulate composites with interfacial thermal resistance. *J. Appl. Phys.* **1997**, *81* (10), 6692–6699. DOI: 10.1063/1.365209.

(50) Park, S.-Y.; Jeong, J.; Shin, H.-C. Geometrical Effect of Active Material on Electrode Tortuosity in All-Solid-State Lithium Battery. *Applied Sciences* **2022**, *12* (24), 12692. DOI: 10.3390/app122412692.

(51) Gomadam, P. M.; Weidner, J. W.; Dougal, R. A.; White, R. E. Mathematical modeling of lithium-ion and nickel battery systems. *J. Power Sources* **2002**, *110* (2), 267–284. DOI: 10.1016/S0378-7753(02)00190-8.

(52) Ebner, M.; Wood, V. Tool for Tortuosity Estimation in Lithium Ion Battery Porous Electrodes. *J. Electrochem. Soc.* **2015**, *162* (2), A3064-A3070. DOI: 10.1149/2.0111502jes.

(53) García-García, R.; García, R. E. Microstructural effects on the average properties in porous battery electrodes. *J. Power Sources* **2016**, *309*, 11–19. DOI: 10.1016/j.jpowsour.2015.11.058.

(54) DeAngelis, F.; Muraleedharan, M. G.; Moon, J.; Seyf, H. R.; Minnich, A. J.; McGaughey, A. J. H.; Henry, A. Thermal Transport in Disordered Materials. *Nanoscale Microscale Thermophys. Eng.* **2019**, *23* (2), 81–116. DOI: 10.1080/15567265.2018.1519004.

(55) Lv, W.; Henry, A. Examining the Validity of the Phonon Gas Model in Amorphous Materials. *Sci. Rep.* **2016**, *6*, 37675. DOI: 10.1038/srep37675. Published Online: Dec. 5, 2016.

(56) Hanus, R. C.; George, J.; Wood, M.; Bonkowski, A.; Cheng, Y.; Abernathy, D. L.; Manley, M. E.; Hautier, G.; Snyder, G. J.; Hermann, R. P. Uncovering design principles for amorphous-like heat conduction using two-channel lattice dynamics. *Mater. Today Phys.* **2021**, *18*, 100344. DOI: 10.1016/j.mtphys.2021.100344.

(57) Bernges, T.; Hanus, R.; Wankmiller, B.; Imasato, K.; Lin, S.; Ghidiu, M.; Gerlitz, M.; Peterlechner, M.; Graham, S.; Hautier, G.; Pei, Y.; Hansen, M. R.; Wilde, G.; Snyder, G. J.; George, J.; Agne, M. T.; Zeier, W. G. Considering the Role of Ion Transport in Diffuson-Dominated Thermal Conductivity. *Adv. Energy Mater.* **2022**, *12* (22), 2200717. DOI: 10.1002/aenm.202200717.

(58) Bernges, T.; Peterlechner, M.; Wilde, G.; Agne, M. T.; Zeier, W. G. Analytical model for two-channel phonon transport engineering. *Mater. Today Phys.* **2023**, *35*, 101107. DOI: 10.1016/j.mtphys.2023.101107.

(59) Huang, M.; Liu, X.; Zhang, P.; Qian, X.; Feng, Y.; Li, Z.; Pan, W.; Wan, C. Thermal conductivity modeling on highly disordered crystalline Y 1−x Nb x O 1.5+x : Beyond the phonon scenario. *Appl. Phys. Lett.* **2021**, *118* (7), 73901. DOI: 10.1063/5.0040546.

(60) Acharyya, P.; Ghosh, T.; Pal, K.; Rana, K. S.; Dutta, M.; Swain, D.; Etter, M.; Soni, A.; Waghmare, U. V.; Biswas, K. Glassy thermal conductivity in Cs3Bi2I6Cl3 single crystal. *Nat. Commun.* **2022**, *13* (1), 5053. DOI: 10.1038/s41467-022-32773-4. Published Online: Aug. 27, 2022.

(61) Di Lucente, E.; Simoncelli, M.; Marzari, N. Crossover from Boltzmann to Wigner thermal transport in thermoelectric skutterudites. *Phys. Rev. Research* **2023**, *5* (3), 33125. DOI: 10.1103/PhysRevResearch.5.033125.

(62) Allen, P. B.; Du, X.; Mihaly, L.; Forro, L. Thermal conductivity of insulating Bi2Sr2YCu2O8 and superconducting Bi2Sr2CaCu2O8: Failure of the phonon-gas

picture. *Phys. Rev. B: Condens. Matter* **1994**, *49* (13), 9073–9079. DOI: 10.1103/PhysRevB.49.9073.

(63) Krauskopf, T.; Pompe, C.; Kraft, M. A.; Zeier, W. G. Influence of Lattice Dynamics on Na+ Transport in the Solid Electrolyte Na3PS4– xSex. *Chem. Mater.* **2017**, *29* (20), 8859–8869. DOI: 10.1021/acs.chemmater.7b03474.

(64) Muy, S.; Schlem, R.; Shao-Horn, Y.; Zeier, W. G. Phonon–Ion Interactions: Designing Ion Mobility Based on Lattice Dynamics. *Adv. Energy Mater.* **2021**, *11* (15), 2002787. DOI: 10.1002/aenm.202002787.

(65) Yang, J.; Wang, Y.; Yang, H.; Tang, W.; Yang, J.; Chen, L.; Zhang, W. Thermal transport in thermoelectric materials with chemical bond hierarchy. *J. Phys.: Condens. Matter* **2019**, *31* (18), 183002. DOI: 10.1088/1361-648X/ab03b6. Published Online: Jan. 31, 2019.

(66) Gupta, M. K.; Ding, J.; Bansal, D.; Abernathy, D. L.; Ehlers, G.; Osti, N. C.; Zeier, W. G.; Delaire, O. Strongly Anharmonic Phonons and Their Role in Superionic Diffusion and Ultralow Thermal Conductivity of Cu7PSe6. *Adv. Energy Mater.* **2022**, *12* (23), 2200596. DOI: 10.1002/aenm.202200596.

(67) Gautam, A.; Sadowski, M.; Ghidiu, M.; Minafra, N.; Senyshyn, A.; Albe, K.; Zeier, W. G. Engineering the Site-Disorder and Lithium Distribution in the Lithium Superionic Argyrodite Li6PS5Br. *Adv. Energy Mater.* **2021**, *11* (5), 2003369. DOI: 10.1002/aenm.202003369.

For table of contents only